ARTICLE

Improved Properties of Oxygen and Argon RF Plasma-Activated Polyester Fabrics Loaded with TiO_2 Nanoparticles

Darka Mihailović,[†] Zoran Šaponjić,[‡] Ricardo Molina,[§] Nevena Puač,[||] Petar Jovančić,[†] Jovan Nedeljković,[‡] and Maja Radetić*[,†]

Textile Engineering Department, Faculty of Technology and Metallurgy, University of Belgrade, Karnegijeva 4, 11120 Belgrade, Serbia, Vinča Institute of Nuclear Sciences, P.O. Box 522, 11001 Belgrade, Serbia, Chemical and Biomolecular Nanotechnology Department, Institut de Química Avançada de Catalunya (IQAC), Consejo Superior de Investigaciones Científicas (CSIC), C/Jordi Girona 18−26, 08034 Barcelona, Spain, and Institute of Physics, Pregrevica 118, 11080 Zemun, Serbia

ABSTRACT The potentials of low-pressure capacitively coupled RF oxygen and argon plasmas for the activation of polyester fibers surface that can enhance the deposition of colloidal TiO_2 nanoparticles were discussed. SEM and XPS analysis confirmed the plasma-induced morphological and chemical changes on the surface of polyester fibers. Oxygen and argon plasma pretreated polyester fabrics loaded with TiO_2 nanoparticles provided maximum reduction of Gram-negative bacteria *E. coli* and UV blocking. The self-cleaning effects tested on blueberry juice stains and photodegradation of methylene blue in aqueous solution proved excellent photocatalytic activity of TiO_2 nanoparticles deposited onto fiber surface. Although both plasmas significantly contributed to overall improvement of properties of such nanocomposite textile material, oxygen plasma treatment, in particular, enhanced the deposition of colloidal TiO_2 nanoparticles and thus ensured superior effects.

KEYWORDS: TiO_2 nanoparticles • PES fabric • oxygen plasma • argon plasma

1. INTRODUCTION

The potentials of plasma for targeted functionalization of different textile materials were extensively studied in last two decades (1). Different plasma-chemical reactions and hence, desirable effects can be obtained by appropriate choice of plasma system and regulation of operating conditions (gas type, gas flow rate, pressure, power, exposure time) (2). Although plasma effects were explored on cellulosic fibers (1, 3−7), the major research so far has focused on imparting the enhanced wettability, dyeability, and printability as well as shrink-resistance and antipilling properties to wool fibers (1, 8−16). The strong hydrophobic nature of some synthetic fibers (polyester, polypropylene) makes adhesion, dyeing, and printing of these materials more complex. The improvement of hydrophilicity of these fibers by the action of reactive and nonpolymerizable plasmas was described in literature in detail (16−19).

The latest studies opened up some new perspectives to plasma that could be utilized for engineering of durable nanocomposite textile materials (20−26). Namely, plasma can activate the surface of different natural and synthetic fibers and hence facilitate the anchoring of metal and metal oxide nanoparticles (NPs). The modification of textile materials with TiO_2 NPs seems to be a viable alternative to conventional finishing processes since small amounts of nanoparticles simultaneously can provide good antibacterial, UV protective and self-cleaning properties. However, the lack of chemical bonding between hydrophobic polyester (PES) fibers and TiO_2 NPs makes the deposition of TiO_2 NPs onto PES fabrics highly challenging (23). The creation of new polar functional groups and particularly carboxylic groups on the PES fiber surface is favorable for the efficient binding of colloidal TiO_2 NPs. Namely, when diameter of nanocrystalline anatase TiO_2 particles becomes smaller than 20 nm, the surface Ti atoms adjust their coordination environment from octahedral to more reactive pentacoordinated (square pyramidal) (27, 28). These undercoordinated defect sites provide improved binding efficiency between carboxylic groups on the fiber surface and Ti atoms.

Recent studies confirmed the positive effects of plasma on the loading of PES fabrics with TiO_2 NPs (22, 23). However, the research so far was oriented toward application of air and oxygen plasmas at low or atmospheric pressures, as the presence of oxygen atoms in the discharge ensure effective plasma oxidation and plasma etching. The aim of this study was to compare the potentials of extremely reactive oxygen and inert argon RF plasmas at low-pressure to activate the PES fiber surface and thus, enhance binding efficiency of the colloidal TiO_2 NPs. The chemical changes on the surface of PES fibers induced by plasma treatment

* Corresponding author. E-mail: maja@tmf.bg.ac.rs.
Received for review March 15, 2010 and accepted May 21, 2010
[†] University of Belgrade.
[‡] Vinča Institute of Nuclear Sciences.
[§] Consejo Superior de Investigaciones Científicas.
[||] Institute of Physics.
DOI: 10.1021/am100209n

Published on Web 06/04/2010

and deposition of TiO_2 NPs were analyzed by XPS. Antibacterial activity of PES fabrics was tested on Gram-negative bacterium *E. coli*. The UV blocking ability was evaluated by determining the UV protection factor (UPF). The photocatalytic activity of TiO_2 NPs deposited onto the PES fabrics was followed by decoloration of blueberry juice stains and methylene blue in aqueous solution under UV illumination.

2. EXPERIMENTAL SECTION

Desized and bleached polyester (PES, 115 g/m^2) woven fabric was cleaned in the bath containing 0.5% nonionic washing agent Felosan RG-N (Bezema) at liquor-to-fabric ratio of 50:1. After 15 min of washing at 50 °C, the fabrics were rinsed once with warm water (50 °C) for 3 min and three times (3 min) with cold water. Subsequently, the samples were dried at room temperature (24).

Glow-discharge treatment of PES fabrics was performed in low-pressure capacitively coupled RF-induced (13.56 MHz) O_2 and Ar plasmas. The power applied to capacitively coupled reactor was 100 W. The treatment time was 2.5 min, the gas flow rate 150 sccm while the pressure was maintained at the constant level of 0.27 mbar. It must be emphasized that our plasma system (29) cannot provide perfect evacuation of air out of the chamber and a small fraction of air remained in the chamber.

The colloid consisting of TiO_2 NPs was synthesized by acid hydrolysis of $TiCl_4$. All the chemicals used for the synthesis of TiO_2 colloid were analytical grade and used as received without further purification (Aldrich, Fluka). Milli-Q deionized water was used as a solvent. The colloid of TiO_2 NPs was prepared in a manner analogous to the procedure proposed by Rajh et al. (30). Four milliliters of $TiCl_4$, cooled to −20 °C, was added dropwise to 200 mL of cooled water (at 4 °C) under vigorous stirring. Obtained clear solution was kept at this temperature for 30 min. The pH value of the solution was in a range 0−1, depending on $TiCl_4$ concentration. Slow growth of the particles was achieved by applying dialysis against 15 times higher volume of water at 4 °C for 3 days until the pH of the solution reached 3.5. Water for dialysis was changed daily. The concentration of TiO_2 colloidal solution was determined from the concentration of the peroxide complex obtained after dissolving the particles in concentrated H_2SO_4 (31). Afterward, the colloid was thermally treated in reflux at 60 °C for 16 h. The synthesized colloid consisted of faceted, single-crystalline, anatase TiO_2 NPs with an average size of about 6 nm (32).

Untreated PES fabric and PES fabrics pretreated with O_2 or Ar plasma were dipped into the 0.1 M TiO_2 colloid (liquor-to-fabric ratio of 1:20) for 5 min and dried at room temperature. After 30 min of curing at 100 °C, the fabrics were soaked twice (5 min) with deionized water and dried at room temperature.

The PES fiber surface morphology before and after plasma treatment was studied by scanning electron microscopy (SEM, JEOL JSM 6460 LV). Gold layer was deposited on the samples before the analysis.

The evaluation of surface chemical changes was carried out by X-ray photoelectron spectroscopy (XPS) analysis. Samples were analyzed using a PHI Model 5500 Multitechnique System with an Al Kα monochromatic X-ray source operating at 350 W. The measurements were conducted under a takeoff angle of 45°. Survey scans were in the range 0−1100 eV, with pass energy of 187.85 eV. High-resolution scans were obtained on the C1s, O1s and Ti2p photoelectron peaks, with pass energy of 23.5 eV. Binding energies were referenced to the C1s photopeak position for C−C and C−H species at 285.0 eV. Surface composition was estimated after a linear background subtraction from the area of the different photoemission peaks modified by their corresponding sensitivity factors (33).

The wettability of the PES fabrics was evaluated by measuring the wetting time according to TEGEWA drop test (34).

The antibacterial efficiency of fabrics was quantitatively evaluated by using the Gram-negative bacterium *Escherichia coli* ATCC 25922. Bacterial inoculum was prepared in the Tripton soy broth (Torlak, Serbia), which was used as the growth medium for bacteria while the physiological saline solution (pH 7.0) was used as the testing medium. Bacteria were cultivated in 3 mL of Tripton soy broth at 37 °C and left overnight (late exponential stage of growth). Afterward, 70 mL of sterile physiological saline solution was added to sterile beaker (400 mL), which was then inoculated with 0.7 mL of the bacterial inoculum. The zero counts were made by removing 1 mL aliquots from the flask with inoculum, and making 1:10 and 1:100 dilutions in physiological saline solution. 0.1 mL of the 1:100 solution was put on the Tripton soy agar (Torlak, Serbia) and after 24 h of incubation at 37 °C, the zero time counts (initial number of bacterial colonies) of viable bacteria were made.

One gram of the sterile PES fabric cut into small pieces was placed into the beaker (70 mL of sterile physiological saline solution inoculated with 0.7 mL of the bacterial inoculum) and shaken for 2 h under UV illumination (TL-D lamp, 18 W, Philips). Two-hour counts were made in accordance with an above-described procedure.

The percentage of bacteria reduction (R, %) was calculated in accordance with eq 1

$$R = \frac{C_0 - C}{C_0} 100 \qquad (1)$$

where C_0 (CFU, colony forming units) is the number of bacterial colonies on the control fabric (fabric without TiO_2 NPs) and C (CFU) is the number of bacterial colonies on the PES fabric loaded with TiO_2 NPs (35, 36).

The UV protection factor (UPF value) of the PES fabrics was determined by UV/vis spectrophotometer Cary 100 Scan (Varian). The UV protection factor (UPF) value was automatically calculated on the basis of recorded data in accordance with Australia/New Zealand standard AS/NZS 4399:1996 using a Startek UV fabric protection application software version 3.0 (Startek Technology).

Laundering durability of antibacterial and UV protective effects was examined after five washing cycles in Polycolor (Werner Mathis AG) laboratory beaker dyer at 45 rpm. The fabrics were washed in the bath containing 0.5% Felosan RG-N (Bezema) at liquor-to-fabric ratio of 40:1. After 30 min of washing at 40 °C, fabrics were rinsed once with warm water (40 °C) for 3 min and three times (3 min) with cold water. The fabrics were subsequently dried at 70 °C (35). The percentage of bacteria reduction after five washing cycles was determined according to eq 1.

The self-cleaning effects were evaluated on the PES fabrics which were stained with blueberry juice. Untreated and plasma pretreated PES fabrics loaded with TiO_2 NPs were cut into 5 × 5 cm^2 pieces and stained with 50 μL of blueberry juice. After drying at room temperature, the fabrics were illuminated using ULTRA-VITALUX lamp (300 W, Osram) for 24 h. The lamp provided sunlike irradiation with a spectral radiation power distribution at wavelengths between 300−1700 nm.

Photocatalytic activity of TiO_2 NPs deposited onto the untreated and plasma pretreated PES fabrics was examined by degradation of methylene blue (MB) in aqueous solution under UV illumination. 0.5 g of PES fabric was immersed in 25 mL of MB solution (10 mg L^{-1}, pH 5.81) and illuminated by ULTRA-VITALUX lamp (300 W, Osram) for 2, 4, 6, 8, and 24 h. The MB

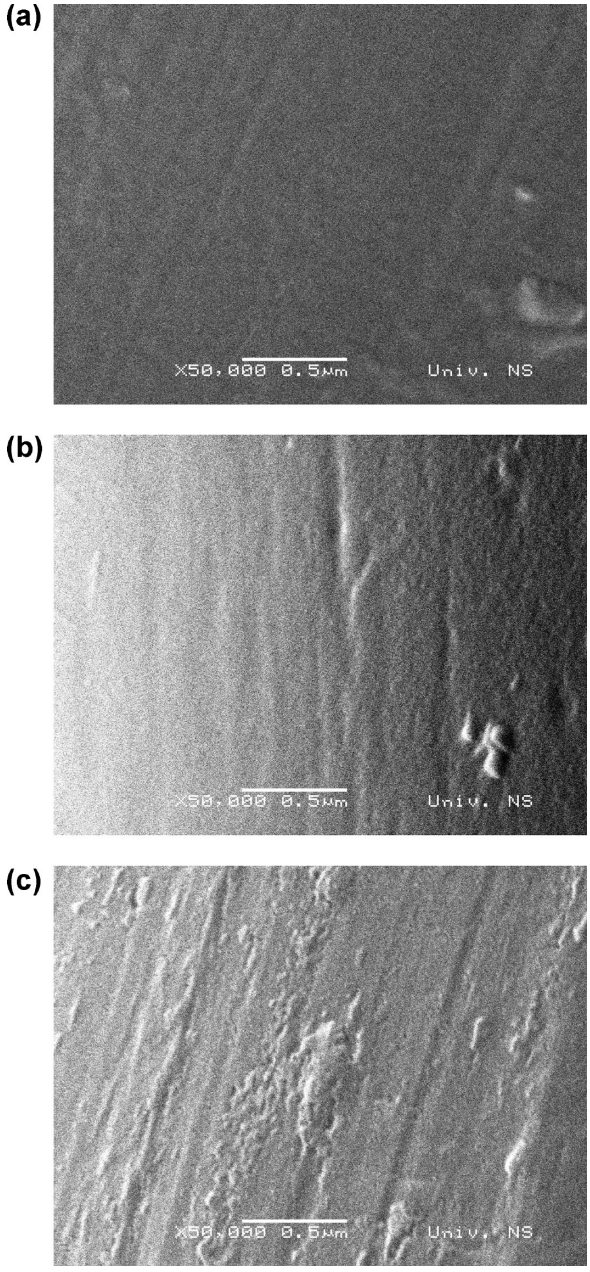

FIGURE 1. SEM images of (a) UPES, (b) O_2PES, and (c) ArPES fibers.

concentration was calculated on the basis of spectrophotometric measurements at 664 nm.

3. RESULTS AND DISCUSSION

Plasma-induced morphological changes of PES fibers were analyzed by SEM. SEM images of untreated (UPES), O_2 plasma-treated (O_2PES), and Ar plasma-treated (ArPES) PES fibers are shown in Figure 1. Figure 1a reveals relatively smooth surface of the UPES fiber. Few striations are visible on the surface of the UPES fiber. Although O_2 plasma treatment led to a formation of small pits and striations (Figure 1b), no significant morphological changes compared to UPES fiber can be observed. On the contrary, Ar plasma produced widened, less-uniform striations (Figure 1c). Additionally, it seems that redeposition of material that was already sputtered from the PES fiber surface during plasma processing occurred. Figure 1c indicates that particularly Ar plasma promoted the increase in fiber surface roughness and consequently, the specific surface area. The topographical changes are due to severe bombardment of PES fibers with energetic plasma particles. It is expected that Ar particles are primarily sputtering the surface away and hence, they induced greater topographical changes. Oxygen particles, however, participate in the chemical etching perhaps supported by ion bombardment, making the fiber surface more even.

Table 1. Elemental Composition of the UPES, O_2PES, and ArPES Fibers

sample	C (at %)	O (at %)	O/C
UPES	80.6	19.4	0.24
O_2PES	74.1	25.9	0.35
ArPES	78.0	22.0	0.28

In addition to morphological properties, plasma action considerably affected the chemical composition of the PES fiber surface. The atomic compositions of PES fibers before and after plasma treatment analyzed by XPS are presented in Table 1. It is noticeable that both O_2 and Ar plasma treatments induced the increase in oxygen content and decrease in carbon content on the PES fiber surface. However, the contribution of O_2 plasma in the generation of oxygen-containing functionalities was more prominent. The O/C atomic ratio that was calculated on the basis of XPS peak intensities, increased by 46% after O_2 plasma treatment and 17% after Ar plasma treatment. Namely, during the O_2 plasma treatment, different plasma species (ions, UV photons and particularly atomic oxygen) may create radicals on the PES fiber surface through polymer scission or hydrogen abstraction (37). The abundance of highly reactive oxygen species in O_2 discharge makes possible rapid reactions with generated radicals on the PES fiber surface and formation of polar oxygen-containing functional groups.

The formation of new oxygen-containing functionalities on the PES fiber surface in Ar plasma was facilitated by the traces of O_2/air in discharge. Even at low concentrations, oxygen is extremely reactive and high rate of its dissociation can be expected. However, Ar ions and UV photons are supposed to be the most responsible for the creation of radicals on the polymer surface (38, 39). In addition to oxygen species in discharge, generated radicals may also react with radicals in neighboring polymer chains, causing the formation of oxidized cross-linked structures on the PES fiber surface. It was suggested that cross-linking reactions obstruct the incorporation of oxygen groups (38, 39) and that can also explain lower content of oxygen on the surface of the Ar plasma treated PES fibers (Table 1). Independently of the applied gas, some of the created radicals also take part in postplasma chemical reactions with the species from surrounding environment. Hence, lower content of oxygen on the surface of the Ar plasma-treated PES fibers can also be due to weaker generation of radicals that further react with atmospheric species.

Deconvolution of high-resolution C1s spectra provided more information on the content of exact oxygen-containing

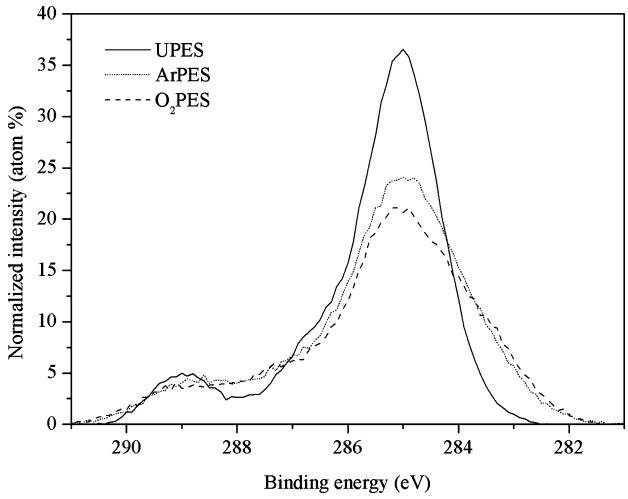

FIGURE 2. High-resolution spectra of C1 photoelectron peaks for the UPES, O_2PES, and ArPES fibers.

Table 2. Relative Intensity Data of Deconvoluted C1s Spectra

	atomic ratio (%)			
sample	C−C, C−H 285.0 eV	C−O 286.6 eV	C═O 288.3 eV	O−C═O 289.1 eV
UPES	77.4	13.1	0.0	9.5
O_2PES	63.6	21.0	8.3	7.1
ArPES	70.4	14.2	10.3	5.1

groups incorporated on the PES fiber surface during the O_2 and Ar plasma treatments. Figure 2 shows the C1s spectra of the UPES, O_2PES and ArPES fibers. The results presented in Table 2 demonstrate that C1s signal of the UPES fibers consists of three peaks at binding energies at 285.0, 286.6, and 289.1 eV, corresponding to carbon atoms in aromatic ring (C−C, C−H), methylene carbons singly bound to oxygen (C−O) and ester carbon atoms (O−C═O), respectively (38−40). In the C1s spectrum of the O_2PES and ArPES fibers additional peak at 288.3 eV related to carbonyl (C═O) group appeared. This observation is in line with literature findings (41). It is also evident that plasma treatment, independently of applied gas, caused the decrease in the percentage of C−C, C−H, and O−C═O groups, and increase in the percentage of C−O groups. The results suggest that newly formed C−O groups and C═O groups are generated at the expense of C−C, C−H, and O−C═O groups (42).

The wetting of PES fabrics was also a sensitive indicator of plasma-induced surface modification. The wetting time of the UPES was 208 s while the O_2PES and ArPES fabrics were wetted within a second. As expected, the wetting time of plasma treated fabrics was significantly shorter. This can be attributed to increased hydrophilicity of plasma treated PES fibers, i.e., implementation of new C═O and C−O groups as well as the presence of considerable amount of O−C═O groups on the PES fibers surface.

Improvement of hydrophilicity along with increased surface roughness made the PES fibers more accessible to hydrophilic colloidal TiO_2 NPs. The effect of plasma action on the deposition of TiO_2 NPs onto PES fabrics was evaluated by XPS. The results of XPS elemental analysis for the

Table 3. Elemental Composition of the UPES, O_2PES, and ArPES Fibers Loaded with TiO_2NPs

sample	C (at %)	O (at %)	Ti (at %)
UPES+TiO_2	79.0	19.7	1.3
O_2PES+TiO_2	59.0	31.9	9.1
ArPES+TiO_2	56.8	37.1	6.1

untreated (UPES+TiO_2), O_2 plasma treated (O_2PES+TiO_2) and Ar plasma-treated (ArPES+TiO_2) PES fibers loaded with TiO_2 NPs are given in Table 3. The high-resolution XPS spectra of Ti2p photoelectron peaks for the UPES+TiO_2, O_2PES+TiO_2, and ArPES+TiO_2 fibers are shown in Figure 3. The $Ti2p_{1/2}$ and $Ti2p_{3/2}$ spin−orbital splitting electrons are located at binding energies of 464.2 and 458.6 eV, respectively. The Ti content on the surface of the O_2PES+TiO_2 and ArPES+TiO_2 fibers was 7 and 4.7 times higher compared to UPES+TiO_2 fabric. It is interesting to note that air plasma treated PES fabrics examined in our previous work, contained almost equal amount of Ti (8.9%) than the O_2PES+TiO_2 fabric (9.1%) (43).

O1s high-resolution spectra of the UPES+TiO_2, O_2PES+TiO_2 and ArPES+TiO_2 fibers are presented in Figure 4. The results in Table 4 demonstrate that O1s signal contain three peaks corresponding to TiO_2 (529.8 eV), C═O (531.6 eV), and C−O (532.9 eV). The existence of the peak at 529.8 eV clearly confirms the presence of TiO_2 NPs on the surface of both PES fibers. Overall XPS results proved that plasma activation of the PES fibers surface positively affected the deposition of TiO_2 NPs.

The antibacterial activity of the UPES+TiO_2, O_2PES+TiO_2 and ArPES+TiO_2 was examined against Gram-negative bacterium *E. coli*. The results of bacteria reduction are presented in Table 5. The control UPES fabric provided bacterial reduction of approximately 1 order of magnitude due to adsorption of *E. coli* on the PES fabric surface (44). The UPES+TiO_2 fabric did not reach the desired level of antibacterial efficiency (R = 99.9%), because the number of bacterial colonies decreased only by 1 order of magnitude compared to control UPES fabric. On the contrary, O_2PES+

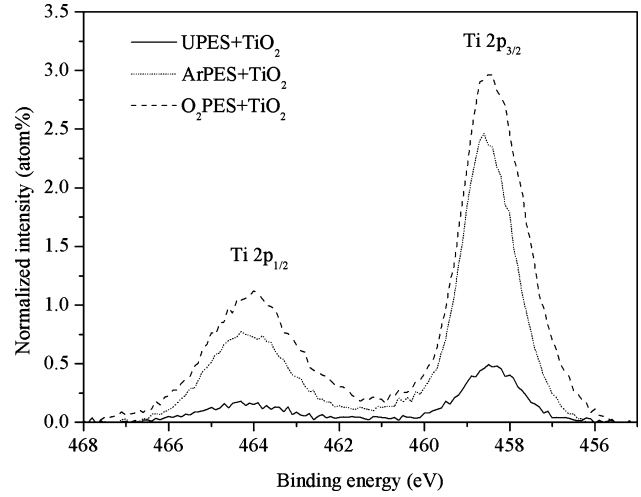

FIGURE 3. High-resolution spectra of Ti2p photoelectron peaks for the UPES+TiO_2, O_2PES+TiO_2, and ArPES+TiO_2 fibers.

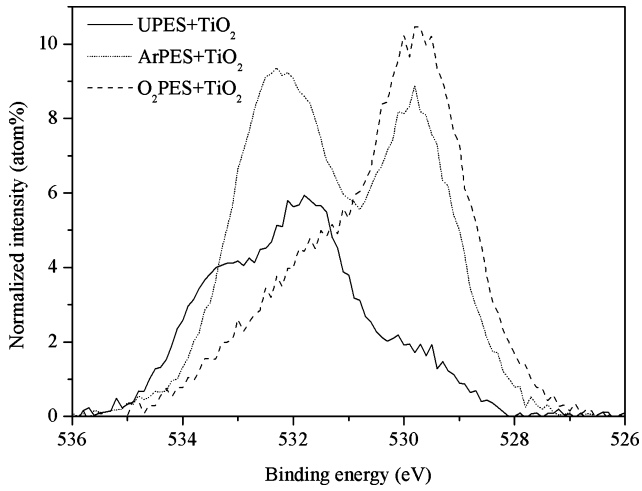

FIGURE 4. High-resolution O1s spectra of the UPES+TiO_2,O_2PES+TiO_2 and ArPES+TiO_2 fibers.

Table 4. Relative Intensity Data of the Deconvoluted O1s Spectra of the UPES+TiO_2, O_2PES+TiO_2, and ArPES+TiO_2 Fibers

	atomic ratio (%)		
sample	TiO_2 529.8 eV	C=O 531.6 eV	C−O 532.9 eV
UPES+TiO_2	18.6	36.9	44.5
O_2PES+TiO_2	70.4	13.8	15.8
ArPES+TiO_2	42.0	35.8	22.2

Table 5. Antibacterial Efficiency of PES Fabrics Loaded with TiO_2 NPs

sample	initial number of bacterial colonies (CFU)	no. of bacterial colonies (CFU)	*R* (%)
UPES		1.5×10^5	
UPES+TiO_2	3.7×10^5	1.3×10^4	91.3
UPES		9.0×10^4	
O_2PES+TiO_2	4.2×10^5	<10	99.9
UPES		1.2×10^4	
ArPES+TiO_2	3.6×10^5	<10	99.9
	After washing		
UPES		9.0×10^4	
O_2PES+TiO_2	4.2×10^5	<10	99.9
UPES		1.9×10^4	
ArPES+TiO_2	6.5×10^5	3.6×10^2	98.1

TiO_2 and ArPES+TiO_2 fabrics provided maximum bacteria reduction, implying that both plasma treatments prior to deposition of TiO_2 NPs had positive influence on antibacterial efficiency. However, the effect of O_2 plasma treatment prior to loading of TiO_2 NPs on the antibacterial efficiency of PES fabrics became more prominent after five washing cycles (Table 5). Apparently, the O_2PES+TiO_2 fabric preserved the initial antibacterial activity, indicating an excellent laundering durability. The antibacterial efficiency of ArPES+TiO_2 fabric slightly decreased after washing, but it was still satisfactory. Higher antibacterial efficiency of the O_2PES+TiO_2 fabric is attributed to a larger amount of TiO_2 NPs deposited onto the O_2 plasma-activated PES fiber surface and likely to higher deposition of TiO_2 NPs.

Table 6. UPF Values of PES Fabric Loaded with TiO_2 NPs

sample	UPF value	std dev	UPF rating
UPES	43.0	0.5	40
O_2PES	42.4	0.6	40
ArPES	42.1	0.6	40
UPES+TiO_2	91.6	17.4	50+
UPES+TiO_2 after washing	66.2	3.7	50
O_2PES+TiO_2	111.3	5.1	50+
O_2PES+TiO_2 after washing	98.2	6.5	50+
ArPES+TiO_2	105.9	4.9	50+
ArPES+TiO_2 after washing	95.6	5.1	50+

The accurate mechanism of bacterial destruction by TiO_2 NPs is not yet fully understood (45). It is supposed that outer membrane of *E. coli* bacteria cells is destroyed by degradation of endotoxin, an integral part of the cell membrane (46). Another approach relies on the "lipid peroxidation" (46, 47). It is assumed that extremely reactive species such as superoxide ions and hydroxyl radicals, generated on the UV irradiated TiO_2 surface, attack the polyunsaturated phospholipids, destroying the bacterial cell membrane. Hence, the interior of the cell and intracellular components become more accessible to TiO_2 nanoparticles and killing of bacteria can be completed because of the loss of essential functions such as respiratory activity (47, 48).

The level of UV protection was quantified and expressed via UPF values that are given in Table 6. The UPES fabric with UPF value of 43 is classified as the fabric with very high UV protection (UPF rating 40). High UPF rating of the UPES fabric is due to the presence of many aromatic rings in macromolecule (49). Plasma treatment did not affect the UV protection properties of the PES fabric. The loading of TiO_2 NPs onto untreated and plasma pretreated PES fabrics led to a significant increase in UPF values. These fabrics are categorized to the group of fabrics that provide maximum UV protection (UPF rating 50+). Large standard deviation of the UPF value measurements for the UPES+TiO_2 fabric (17.4) could be due to uneven distribution of TiO_2 NPS on the fiber surface. The O_2PES+TiO_2 fabric exhibited the best UPF protection. The larger the amount of deposited TiO_2 NPs, the more efficient the UV blocking. Although UPF values of the O_2PES+TiO_2 and ArPES+TiO_2 fabrics slightly decreased after five washing cycles, the UPF rating of 50+ was maintained. Even after washing, these samples provided better UV protection than the UPES+TiO_2 fabric before washing. The UPF value of the UPES+TiO_2 fabric decreased after washing and its UPF rating dropped down to 50.

The effect of TiO_2 NPs on the self-cleaning properties of PES fabrics was examined by decoloration of blueberry juice stains. The images of PES fabrics were recorded immediately after blueberry juice staining (zero time of illumination) and after 24 h of UV illumination (Figure 5). It can be observed that initial color of blueberry juice stain on the UPES fabric differs from the PES fabrics loaded with TiO_2 NPs. In addition to color difference, blueberry juice stains on the O_2PES+TiO_2 and ArPES+TiO_2 fabrics were more spread over. Figure 5 clearly reveals that after 24 h of UV illumination, the

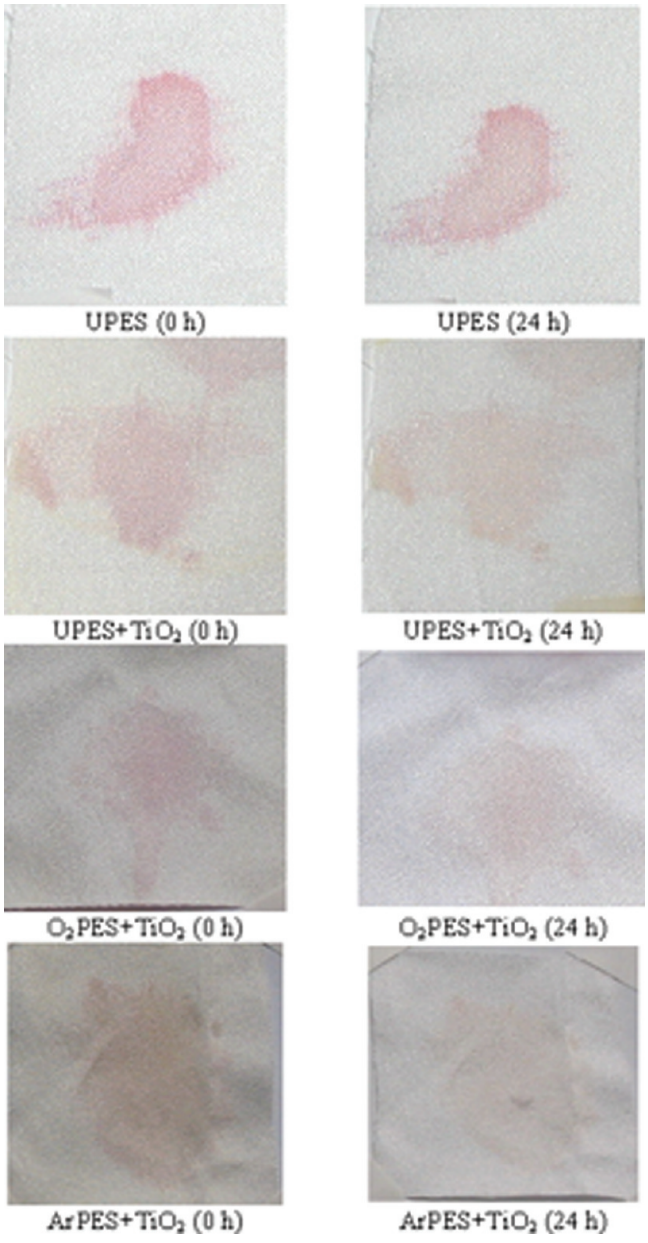

FIGURE 5. Blueberry juice stains on the UPES fabric and PES fabrics loaded with TiO_2 NPs before and after 24 h of UV illumination.

blueberry juice stain on the UPES fabric remained intact. On the contrary, PES fabrics loaded with TiO_2 NPs provided eye visible stain decoloration. These samples became lighter and less red. As predicted, self-cleaning efficiency was the most pronounced on the O_2PES+TiO_2 fabric.

Photocatalytic activity of TiO_2 NPs deposited onto the PES fabrics was also studied by decoloration of dye methylene blue (MB) in aqueous solution under the UV illumination. Figure 6 presents the dependence of C/C_0 versus time of UV illumination for the UPES, UPES+TiO_2, O_2PES+TiO_2, and ArPES+TiO_2 fabrics. It is evident that MB concentration in contact with the UPES fabric slightly decreased in the first 6 h of UV illumination and after that remained unchanged. The detected change in MB concentration is due to adsorption of dye on the UPES fabric.

After 24 h of UV illumination, only about 75% of MB was removed from the solution in contact with the UPES+TiO_2 fabric. However, after multiple rinsing in water the UPES+TiO_2 fabric remained pale blue, demonstrating that complete photodegradation of MB was not obtained neither in MB solution nor on the fabric.

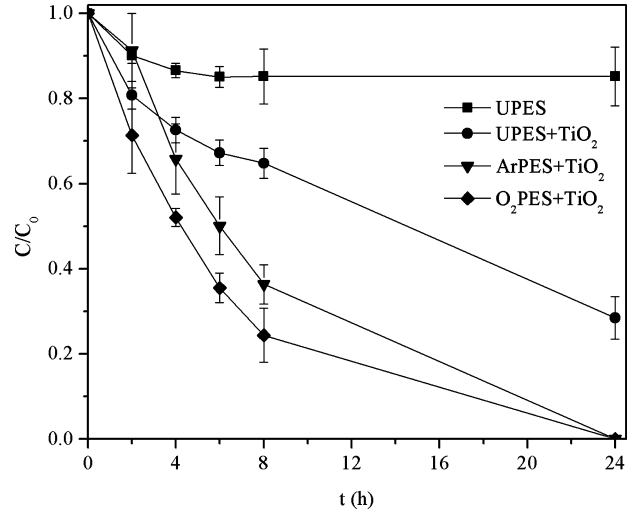

FIGURE 6. MB photodegradation by TiO_2 nanoparticles on differently modified PES fabrics under UV illumination.

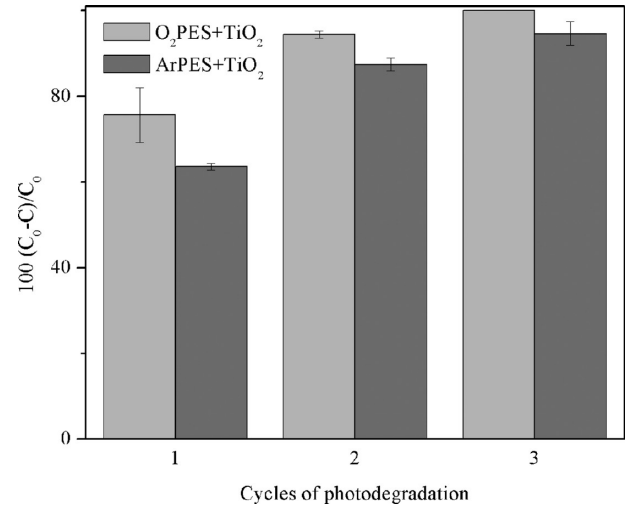

FIGURE 7. Changes in relative concentration of MB solution after repeated photodegradation processes under the UV illumination (8 h) for the O_2PES+TiO_2 and ArPES+TiO_2 fabrics.

The O_2PES+TiO_2 and ArPES+TiO_2 fabrics induced complete removal of MB from the solution after 24 h of UV illumination. These fabrics remained white, proving the total photodegradation of MB. The results also indicate that the O_2PES+TiO_2 fabric ensured the highest rate of MB photodegradation.

To investigate the durability of photocatalytic activity of TiO_2 NPs deposited onto plasma pretreated PES fabrics, the photodegradation process was repeated two more times. The MB solution was completely decolorized in contact with the O_2PES+TiO_2 and ArPES+TiO_2 fabrics after 24 h of UV illumination also in the second and the third photodegradation cycle. Photodegradation rate increased in each subsequent cycle (Figure 7). Such trend was also observed on the same PES fabrics that were corona treated prior to loading of TiO_2 NPs (26). Similar results were also reported by other

researches (50). Higher photocatalytic activity of TiO_2 NPs in repeated cycles is suggested to be due to surface cleaning from impurities during the first cycle. Again, the O_2PES+ TiO_2 fabric exhibited superior photodegradation ability, i.e., the total MB removal in the third photodegradation cycle was obtained already after 8 h of UV illumination.

4. CONCLUSIONS

Oxygen and argon RF plasmas successfully activated the surface of PES fabrics, inducing the enhanced deposition of colloidal TiO_2 nanoparticles. XPS measurements confirmed higher Ti content on the plasma pretreated PES fiber surfaces. This was especially pronounced on the PES fabrics activated with oxygen plasma. Oxygen and argon plasma pretreated PES fabrics loaded with TiO_2 nanoparticles ensured excellent antibacterial activity against Gram-negative bacterium *E. coli* and maximum UV protection. In particular oxygen plasma pretreated PES fabrics loaded with TiO_2 nanoparticles exhibited good laundering durability of obtained effects. TiO_2 nanoparticles deposited on the PES fabrics ensured efficient photodegradation of methylene blue in aqueous solution and blueberry juice stains under the UV illumination. Although oxygen plasma pretreated PES fabrics loaded with TiO_2 NPs demonstrated higher overall efficiency, the effects provided by the PES fabrics pretreated with argon plasma were excellent.

Acknowledgment. The financial support for this work was provided by the Ministry of Science of Republic of Serbia (Projects TR 19007 and 142066). We gratefully acknowledge M. Bokorov (University of Novi Sad, Serbia) for performing SEM measurements. Authors also acknowledge Dr. Jordi Esquena for the XPS analysis and the Spanish Ministry of Science and Innovation (CTQ2008-06892-C03-01 project).

REFERENCES AND NOTES

(1) *Plasma Technologies for Textile*; Shishoo, R., Ed.; Woodhead Publishing Limited: Cambridge, U.K., 2007.
(2) Grill, A. *Cold Plasma in Materials Fabrication: From Fundamentals to Application*; IEEE Press: New York, 1994.
(3) Boenig, H. V. *Plasma Science and Technology*; Cornell University Press: London, 1982.
(4) Cai, Z.; Qiu, Y.; Zhang, C.; Hwang, Y. H.; McCord, M. *Text. Res. J.* **2003**, *73*, 670–674.
(5) Rashidi, A.; Moussavipourgharbi, H.; Mirjalili, M.; Ghoranneviss, M. *Indian J. Fibre Text. Res.* **2004**, *29*, 74–78.
(6) Navaneetha Pandiyaraj, K.; Selvarajan, V. *J. Mater. Process Technol.* **2008**, *199*, 130–139.
(7) Karahan, H. A.; Özdoğan, E. *Fiber Polym.* **2008**, *9*, 21–26.
(8) Molina, R.; Jovančić, P.; Jocić, D.; Bertran, E.; Erra, P. *Surf. Interface Anal.* **2003**, *35*, 128–135.
(9) Rakowski, W. *Fibres Text. East Eur.* **1995**, *3*, 45–49.
(10) Hesse, A.; Thomas, H.; Höcker, H. *Text. Res. J.* **1995**, *65*, 355–361.
(11) Zuchairah, I. M.; Pailthorpe, M. T.; David, S. K. *Text. Res. J.* **1997**, *67*, 69–74.
(12) Kan, C. W.; Yuen, C. W. M. *J. Appl. Polym. Sci.* **2006**, *102*, 5958–5964.
(13) Kan, C. W.; Yuen, C. W. M. *Plasma Processes Polym.* **2006**, *3*, 627–635.
(14) Canal, C.; Erra, P.; Molina, R.; Bertran, E. *Text. Res. J.* **2007**, *77*, 559–564.
(15) Morent, R.; De Geyter, N.; Verschuren, J.; De Clerk, K.; Kiekens, P.; Leys, C. *Surf. Coat. Technol.* **2008**, *202*, 3427–3449.
(16) Ueda, M.; Tokino, S. *Rev. Prog. Color.* **1996**, *26*, 9–19.
(17) Raffaele-Addamo, A.; Riccardi, C.; Selli, E.; Barni, R.; Piselli, M.; Poletti, G.; Orsini, F.; Marcandalli, B.; Massafra, M. R.; Meda, L. *Surf. Coat. Technol.* **2003**, *174*−*175*, 886–890.
(18) Masaeli, E.; Morshed, M.; Tavanai, H. *Surf. Interface Anal.* **2007**, *39*, 770–774.
(19) Leroux, F.; Campagne, C.; Perwuelz, A.; Gengembre, L. *Surf. Coat. Technol.* **2009**, *203*, 3178–3183.
(20) Yuranova, T.; Rincon, A. G.; Bozzi, A.; Parra, S.; Pulgarin, C.; Albers, P.; Kiwi, J. *J. Photochem. Photobiol., A* **2003**, *161*, 27–34.
(21) Bozzi, A.; Yuranova, T.; Guasaquillo, I.; Laub, D.; Kiwi, J. *J. Photochem. Photobiol., A* **2005**, *174*, 156–164.
(22) Bozzi, A.; Yuranova, T.; Kiwi, J. *J. Photochem. Photobiol., A* **2005**, *172*, 27–34.
(23) Qi, K.; Xin, J. H.; Daud, W. A. *Int. J. Appl. Ceram. Technol.* **2007**, *4*, 554–563.
(24) Radetić, M.; Ilić, V.; Vodnik, V.; Dimitrijević, S.; Jovančić, P.; Šaponjić, Z.; Nedeljković, J. M. *Polym. Adv. Technol.* **2008**, *19*, 1816–1821.
(25) Mejia, M. I.; Marin, J. M.; Restrepo, G.; Pulgarin, C.; Mielczarski, E.; Mielczarski, J.; Arroyo, Y.; Lavnchy, J. C.; Kiwi, J. *Appl. Catal., B* **2009**, *91*, 481–488.
(26) Mihailović D.; Šaponjić Z.; Radoičić M.; Molina R.; Radetić T.; Jovančić P.; Nedeljković J.; Radetić M. *Polym. Advan. Technol.* **2010**, in press.
(27) Chen, L. X.; Rajh, T.; Jäger, W.; Nedeljković, J.; Thurnauer, N. C. *J. Synchrotron Radiat.* **2002**, *6*, 445–447.
(28) Rajh, T.; Chen, L. X.; Lukas, K.; Liu, T.; Thurnauer, M. C.; Tiede, D. M. *J. Phys. Chem. B* **2002**, *106*, 10543–10552.
(29) Radetić, M.; Puač, N.; Jovančić, P.; Šaponjić, Z.; Petrović, Z. Lj *Text. Res. J.* **2009**, *79*, 558–565.
(30) Rajh, T.; Ostafin, A.; Mićić, O. I.; Tiede, D. M.; Thurnauer, M. C. *J. Phys. Chem.* **1996**, *100*, 4538–4545.
(31) Thompson, R. C. *Inorg. Chem.* **1984**, *23*, 1794–1798.
(32) Mihailović, D.; Šaponjić, Z.; Radoičić, M.; Radetić, T.; Jovančić, P.; Nedeljković, J.; Radetić, M. *Carbohydr. Polym.* **2010**, *79*, 526–532.
(33) Wagner, C. D.; Davis, L. E.; Zeller, M. V.; Taylor, J. A.; Raymond, R. M.; Gale, L. H. *Surf. Interface Anal.* **1981**, *3*, 211–225.
(34) Schmidt, G.; Wurster, P. *Melliand Int.* **1987**, *68*, 581–583.
(35) Lee, H. J.; Yeo, S. Y.; Jeong, S. H. *J. Mater. Sci.* **2003**, *38*, 2199–2204.
(36) Ki, H. Y.; Kim, J. H.; Kwon, S. C.; Jeong, S. H. *J. Mater. Sci.* **2007**, *42*, 8020–8024.
(37) Riccardi, C.; Barni, R.; Selli, E.; Mazzone, G.; Massafia, M. R.; Marcandalli, B.; Poletti, G. *Appl. Surf. Sci.* **2003**, *211*, 386–397.
(38) Morent, R.; De Geyter, N.; Leys, C.; Gengembre, L.; Payen, E. *Surf. Coat. Technol.* **2007**, *201*, 7847–7854.
(39) Morent, R.; De Geyter, N.; Leys, C.; Gengembre, L.; Payen, E. *Text. Res. J.* **2007**, *77*, 471–488.
(40) Ben Amor, S.; Jacquet, M.; Fioux, P.; Nardin, M. *Appl. Surf. Sci.* **2009**, *255*, 5052–5061.
(41) De Geyter, N.; Morent, R.; Leys, C. *Surf. Coat. Technol.* **2006**, *201*, 2460–2466.
(42) Molina, R.; Espinós, J. P.; Yubero, F.; Erra, P.; González-Elipe, A. R. *Appl. Surf. Sci.* **2005**, *252*, 1417–1429.
(43) Mihailović D.; Šaponjić Z.; Molina R.; Radoičić M.; Esquena J.; Jovančić P.; Nedeljković J.; Radetić M., submitted.
(44) Yuranova, T.; Rincon, A. G.; Bozzi, A.; Parra, S.; Pulgarin, C.; Albers, P.; Kiwi, J. *J. Photochem. Photobiol., A* **2003**, *161*, 27–34.
(45) Robertson, P. K. J.; Bahnemann, D. W.; Robertson, J. M. C.; Wood, F. In *The Handbook of Environmental Chemistry*; Springer: New York, 2005; Vol. 2, subsection M; pp 367−423.
(46) Sunada, K.; Kikuchi, Y.; Hashimoto, K.; Fijishima, A. *Environ. Sci. Technol.* **1998**, *32*, 726–728.
(47) Maness, P. C.; Smolinski, S.; Blake, D. M.; Huang, Z.; Wolfrum, E. J.; Jacoby, W. A. *Appl. Environ. Microbiol.* **1999**, *65*, 4094–4098.
(48) Huang, Z.; Maness, P. C.; Blake, D. M.; Wolfrum, E. J.; Smolinski, S. L.; Jacoby, W. A. *J. Photochem. Photobiol., A* **2000**, *130*, 163–170.
(49) Gorenšek, M.; Bukošek, V. *Acta Chim. Slov.* **2006**, *53*, 223–228.
(50) Uddin, M. J.; Cesano, F.; Bonino, F.; Bordiga, S.; Spoto, v.; Scarano, D.; Zecchina, A. *J. Photochem. Photobiol., A* **2007**, *189*, 286–294.

AM100209N